Geological Quarterly, 2003, **47** (1): 1–12

Use of geomechanical research in the conservation of stone monuments (Maadi Town Temple, Fayoum, Egypt)

Joanna PINIŃSKA and Hemdan Rabbie ATTIA

Pinińska J. and Attia H. R. (2003) — Use of geomechanical researches in the conservation of stone monuments (Maadi Town Temple, Fayoum, Egypt). Geol. Quart., **47** (1): 1–12. Warszawa.

Maadi Town Temple was discovered by Prof. Villiano of Milan University in 1936, during excavation work in the Maadi Town area of the Fayoum Province. Since this discovery there has been no scientific ally based conservation of the monument, often than some unsuccessful restoration. The ruins were left uncovered and exposed to climatic deterioration until 1994, when scientific members of the Faculty of Archaeology of Cairo University undertook a study of the degradation processes affecting the Temple. This started with field-based observation of the monument's condition and, description of the building materials, (limestone and mortar). In 1997 samples of the building material were collected on site and in 1998 laboratory studies of those samples were carried out in the Department of Geomechanics at the Warsaw University. The laboratory studies comprised two main steps: diagnosis of the deterioration factors and their geomechanical interpretation as an effect of salt solution, water saturation and temperature changes. The behaviour of building limestone and mortar were considered relative to their mineralogical composition, internal structure and path of deformation. In laboratory testing two geomechanical methods were used: non- destructive ultrasonic control and destructive uniaxial compression testing with monitoring of prefailure and postfailure deformation fabrics. Both applied methods showed the salt solutions to be the main deterioration factor affecting the stone elements and the anisotropy and various properties of the mortar and of the bedded limestone as the main factors destabilising the construction of the Temple as a whole. Degradation occurs gradually due to the internal and external inhomogeneous field of deformation caused by climatic changes, with cyclic strengthening due to salt incrustation and subsequent softening after water saturation and temperature changes.

Joanna Pinińska, Faculty of Geology, Warsaw University, Żwirki i Wigury 93, PL-02-089 Warszawa, Poland; e-mail: ihigi@geo.uw.edu.pl; Hemdan Rabbie Attia, Faculty of Archeology, Cairo University, Giza, Egypt *(received: December 14, 2001; accepted: March 21, 2002).*

Key words: strength, degradation, conservation, monuments, rocks.

INTRODUCTION

The Maadi Town Temple was built by Amenmehat III and IV (Hewisan, 1986) and during the Ptolemic and Roman periods some halls and statues were added at the front of the Temple (Wolfgang and Eberhard, 1979; Helmi and Attia 1996; Abd El-Hady, 2000). The regional geology comprises Tertiary and Quaternary deposits (Beadnell, 1905; Said, 1962).

The Maadi Town Temple was built of calcareous rocks from nearby quarries. The stone blocks were probably derived from outcrops of Eocene rocks located in the Gabal Qotruni along the north periphery of the Lake Qarun at the northern periphery of the Fayoum Depression (Attia, 1995). These are bright yellow limestones, generally hard, partly marly or sandy, with fossils, mostly mollusc shells, nummulites and corals (Pinińska and Attia, 1999*a*, *b*).

The recent condition of the Temple is poor because of deterioration caused by micro and macro cracks, exfoliation, fall of mortar fragments and wind corrosion. Those processes were accelerated when the ruins were excavated out of their sand cover and exposed to climatic deterioration, and this was compounded when, at early stage of conservation, misguided restoration with the use of Portland cement was attempted (Fig. 1a, b).

The substrate on which the Temple stands does not affect the monument mechanically and its deterioration depends mostly on climatic factors.

The main deterioration factors are humidity, varying temperature, wind action and salt solution. Additional manmade

Fig. 1. General view of the Maadi Town Temple

a — temple left without sandy cover for the half of the Century, b — examples of deterioration: macrocracks, exfoliation and fall of mortar of statues an walls

damage was caused by criminal activity, ill will or lack of knowledge or lack of competence in attempts at imposing preservation measures.

Atmospheric humidity exceeds 76% at nights and salts — mostly halite — dispersed in pores of the Temple stones become diluted. During the day, the water evaporates from the salt solutions, causing re-crystallisation of the halite and other diluted salts. These processes are repeated in daily and seasonal cycles, leading to mechanical destruction of the internal structure of the building stones and mortar. Partially disintegrated material becomes open to corrosive action of wind and other agents.

Thermal expansion and contraction causes development of new microcracks and further opens existing ones, and in the presence of increased humidity an exfoliation develops.

BASIC PROPERTIES OF THE CONSTRUCTION MATERIALS

Samples of building material from the Maadi Town Temple, i.e. limestone and mortar were subjected to laboratory studies. Their mineral composition and their physical, mechanical and thermal properties both in their natural state and after exposition to different agents of deterioration — such as salt solution, and temperature cycles — were determined.

Analysis by polarising microscope, X-ray diffraction and scanning electron microscope (SEM) methods showed that the limestone is essentially composed of calcite and a small amount of halite, gypsum and quartz, while the mortar is essentially

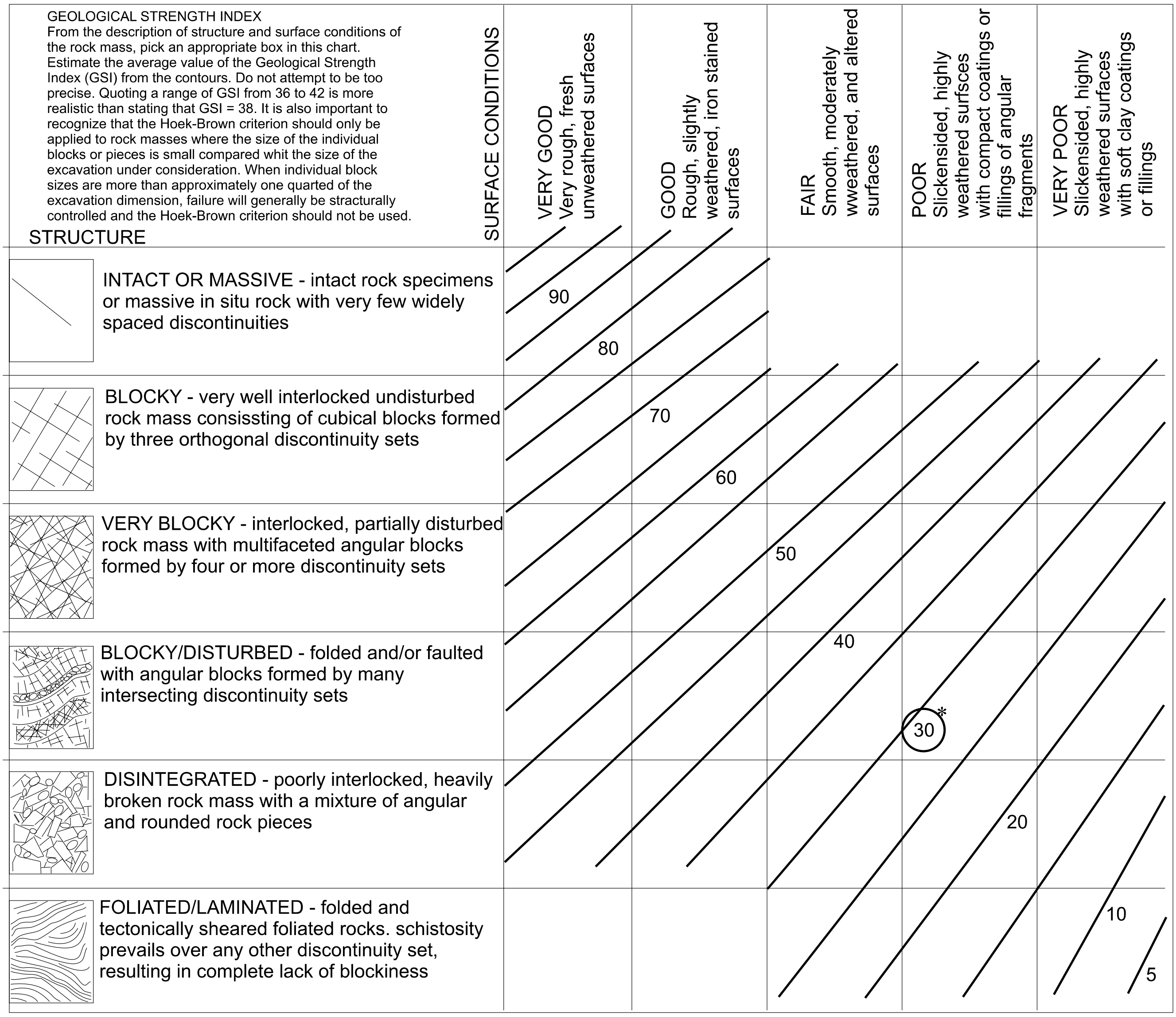

Fig. 2. Characterisation of rock masses on the basis of interlocking and joint alteration (adjusted from Hoek, 1994) after Hoek and Marinos (2001)

5–90 — GSI values, * — GSI value for Maadi Town limestone classification

composed of gypsum, which partially was converted to anhydrite due to the effect of elevated temperatures.

The density of the limestone is 2.17 Mg/m^3, the porosity 19%, and the water absorption about 5.93%. After crystallisation of the salt solutions the density of the limestone decreases and the porosity increases. The susceptibility of limestone to water absorption significantly increased as an effect of temperature cycles. The uniaxial compressional strength of the limestone in its natural state ranges from 24 to 35 MPa, while elasticity properties are low: e.g. The modulus of elasticity E is < 8 GPa and the phases of linear elasticity are short.

In general, the limestone used for construction of the Maadi Town Temple, according to the Geological Strength Index (in: Hoek and Marinos, 2001), may be classified as a rock with a value of 30 GSI (Fig. 2).

GEOMECHANICAL MODELLING OF THE DETERIORATION PROCESSES

After the most important deterioration processes were defined: salt solutions, impact of water and temperature cycles, modelling was performed on specially prepared samples according to the standards needed for uniaxial compression strength tests.

The following conditions were modelled:

— **salt solution cycles**: samples were alternately submerged into a salt solution and then dried. At the end of the first salt solution cycle white spots formed on the surface of the samples and continued their development during further cycles. Such growth of halite crystals on the surface of building walls or on a rock surface is known as efflorescence.

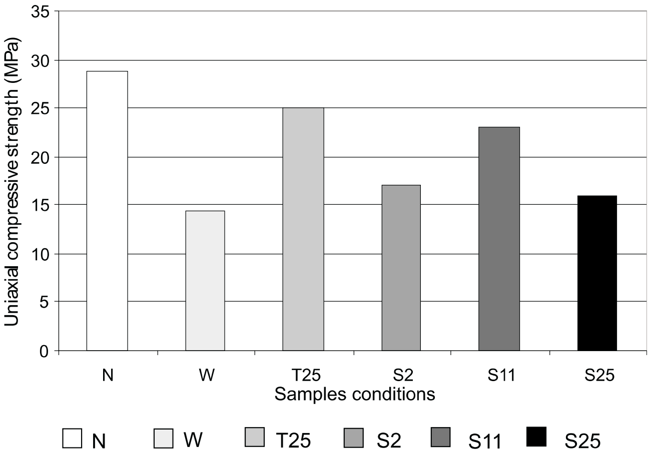

Fig. 3. Diagram of uniaxial compressive strength R_c of limestone samples in natural state (N) and after the impact in deterioration factors: W — water impact, T25 — temperature cycles, S2, S11, S25 — salt solution cycles

— **impact of water**: samples were submerged in water for 168 hours at a temperature of approximately 20°C. A small part of the calcium carbonate content of the limestone samples was dissolved, salts were leached from the pores and the weight of the samples increased due to water absorption.

— **temperature cycles**: samples were alternately subjected to high and low temperatures ranging from 5 to 60°C in 25 temperature cycles. During the temperature cycles microcracks and macrocracks appeared, as well brown and yellow spots on the limestone sample surfaces, which are varied in their shapes and hue.

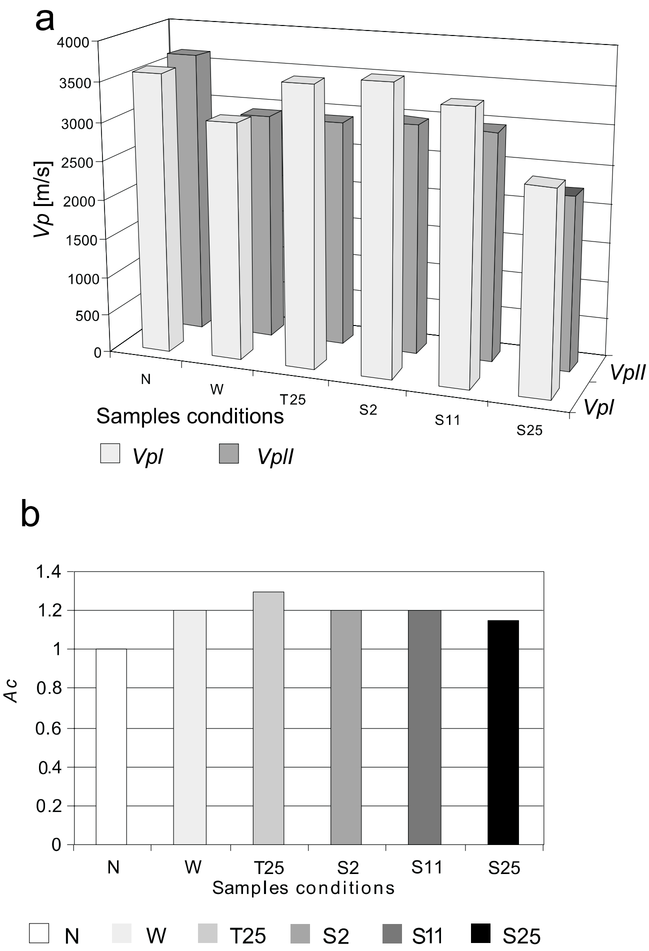

Fig. 4. Diagram of ultrasonic longitudinal waves velocity (V_p)

a — perpendicular (Vp_I) and parallel (Vp_{II}) to the layers of limestone samples; b — acoustic anisotropy coefficient (Ac) for Vp in natural state and after the impact of deterioration factors; for other explanations see Fig. 3

RESULTS OF MODELLING

Changes in both the velocity of longitudinal waves and the compression strength were analysed to provide a measure of the rock changes (Figs. 3 and 4).

LONGITUDINAL WAVE VELOCITY

After the first cycle of salt solution, the longitudinal waves (Vp) increased in a direction perpendicular to the sedimentary layers (Vp_I) and decreased in a direction parallel to the layers (Vp_{II}). This anisotropy increased, probably, due to halite crystals precipitating along sedimentary laminae and causing breaking of interlayer bonds.

After the second cycle of salt solution, the longitudinal wave velocity also decreased in a direction perpendicular to the layers; the decrease in velocity continued further continued and varied as a consequence of cyclic crystallization of salts and development of cracks in and crumbling of massive rock material during subsequent cycles in all samples as shown in Figure 5.

After 12 hours of immersion in water the longitudinal wave velocity (Vp) in limestone samples decreased. After 24 hours, the rate of decrease in the longitudinal wave velocity perpendicular to layering (Vp_I) became semi-stable, while the longitudinal wave velocity parallel to layering (Vp_{II}) continued to decrease as shown in Figure 6.

After the first temperature cycle, the velocity of longitudinal waves (Vp) increased in both major directions, but after the second cycle the longitudinal wave velocity decreased and continued its fall at a variable rate during subsequent cycles. The variable decrease in the velocity was a consequence of thermal expansion and contraction, which lead to development of micro cracks and disintegration by crumbling.

The velocity decrease in the longitudinal waves became semi-stable during the last 7 cycles of temperature changes in a direction perpendicular to the layers (Vp_I), and during the last 5 cycles in a direction parallel to the layers (Vp_{II}) of limestone samples as shown in Figure 7.

As a result of the testing it was noted that the longitudinal wave velocity values (Vp) of the Temple construction limestone generally decreased in all directions under the impact of deterioration factors and after impact of 25 temperature change cycles velocity decreased by 1% only. But velocity parallel to layers (Vp_{II}) dropped immediately, therefore the coefficient of acoustic

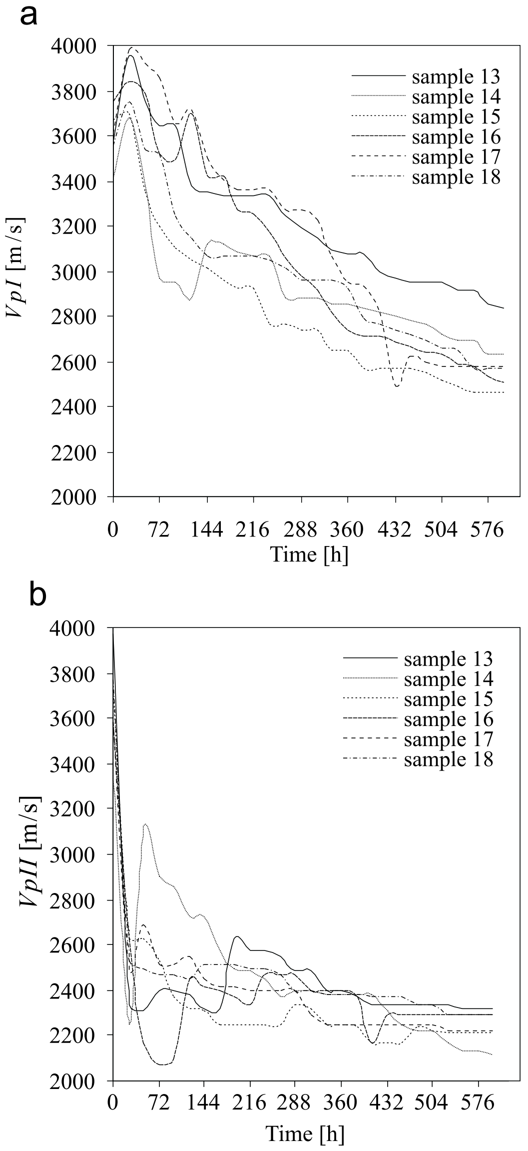

Fig. 5. Changes of ultrasonic longitudinal waves velocity (Vp)

a — perpendicular (Vp_I), b — parallel (Vp_{II}) to the layers after impact of solution cycles

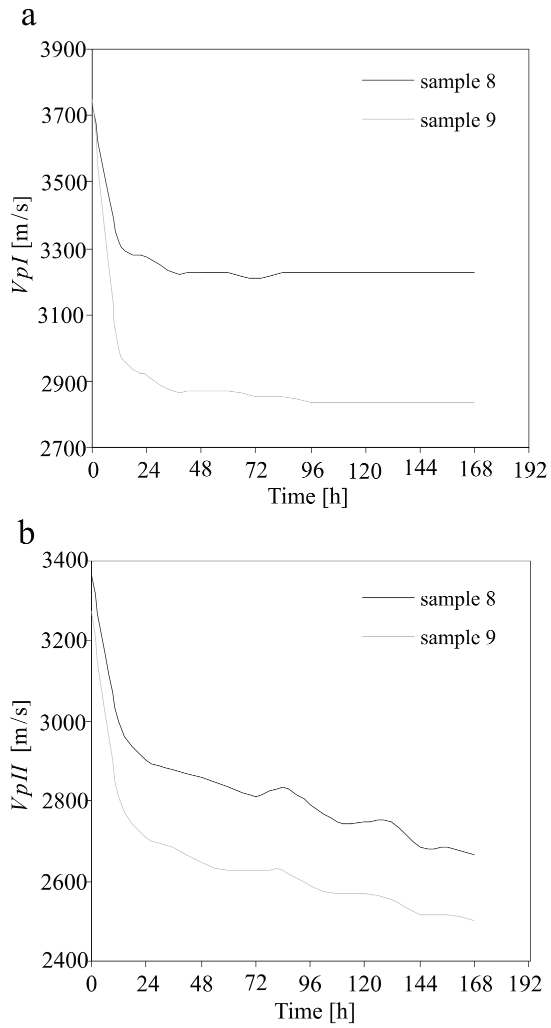

Fig. 6. Changes of ultrasonic longitudinal waves velocity (Vp)

a — perpendicular (Vp_I), b — parallel (Vp_{II}) to the layers after impact of immersion in water

anisotropy (Ac) of the longitudinal waves (Vp) increased after the effect of the deterioration factors due to greater decay parallel to layering than in a perpendicular direction.

The latter noticeably reduced the resistance of the stone material.

COMPRESSION STRENGTH

Generally, after the impact of deterioration factors, the Geological Strength Index (GSI) fell to a value of 20.

The complete, prefailure and postfailure curves of deformation in the natural state show, within the tested limestone, that the complexity of the fracturing process (Fig. 8a). agreed well with model IV of the deformation path common for weak calcareous rocks (Pinińska, 1995, 1999). The prefailure phases are slightly defined and, after the pick point, deformation curves descend monotonically with segments of very irregular macro- and micro-oscillations. The oscillations trace the complex fracturing processes interrelated with a short part of the strengthening processes. After the stress drops to 60% of the maximum stress value, the curves descend with very small pulses. For the final part of the postfailure deformation, a specific characteristic is that the high residual strength value (Fig. 8b) ranges over 20% of total uniaxial compression strength (R_c).

The prefailure deformation phases in the natural state are characterised by a small amount of compaction (I) — at values up to 5 Mpa, then full linear deformation up to 10 Mpa (II) and then shortly afterwards, there start phases of initial, brittle fracturing (III) and stable fracturing (IV) which change, at a value of 60% of total compression strength (R_c), to phases of unstable deformation (V). The critical axial strain (E_z) range interval between 0.2 and 0.4%, critical circumferential strain range up to 0.49% and volumetric range up to 0.58% (Fig. 8c).

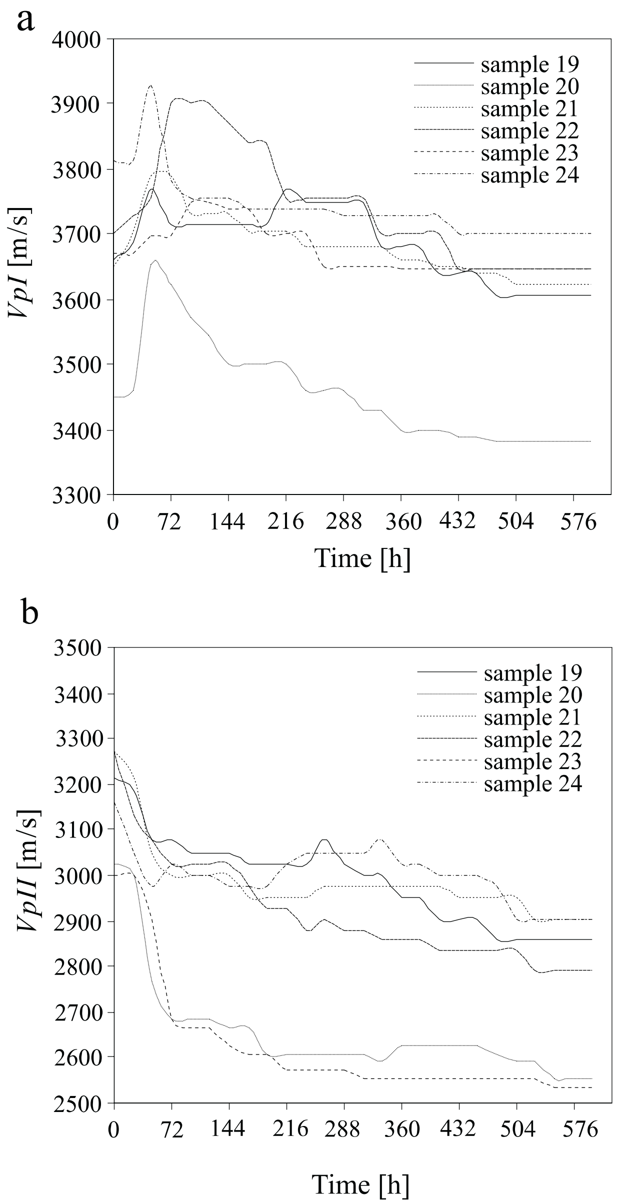

Fig. 7. Changes of ultrasonic longitudinal waves velocity (V_p)

a — perpendicular (Vp_I), b — parallel (Vp_{II}) to the layers after impact of temperature cycles

The fracturing processes show various reactions to the deterioration factors.

The immersion in water makes the limestone much softer. But although the total compression strength (R_c) becomes lower, the final postfailure high residual strength value, ranging to 20% of total compression strength (R_c), is maintained. Yet the process of stable and unstable cracking become smoother. The irregular macro and micro oscillations are visible close to the pick point of deformation only (Fig. 9a). Then the deformation path descends gradually with rare symptoms of irregular displacement, what means that the brittle cracking has stopped (Fig. 9b).

The prefailure deformation phases after immersion in water are characteristically by smaller than in the natural state the phase of compaction (I) — ranging up to 4 Mpa, then full linear deformation up to 8 Mpa (II), a shortening of phases of initial, brittle fracturing (III) and widening of phases of stable fracturing (IV). Therefore the phases of unstable deformation (V) appearing at 13 Mpa, range to over 70% of total compression strength (R_c). The critical axial strain (E_z) and critical circumferential strain increase. Particular increases were seen in the volumetric strain, in ranging after the impact of water up to 0.70% (Fig. 9c).

The impact of temperature shows many similarities in shape with those of water impact but the degradation in strength is very low (Fig. 10a). The path of deformation is very smooth and the irregular macro and micro oscillations near the pick point disappear. The deformation path descends gradually without symptoms of irregular displacement and residual strength ranges over 20% of total compression strength (R_c) are maintained (Fig. 10b).

The prefailure deformation phases after the effect of temperature are characterised by phase of compaction (I) — ranging up to 7 Mpa, then full linear deformation up to 11 Mpa (II) and then short phases of initial, brittle fracturing (III) and phases of stable fracturing (IV). The phase of unstable deformation (V) appears at 18 Mpa and range close to 80% of total compression strength (R_c). Yet the critical axial strain (E_z), critical circumferential strain and especially volumetric strain are high as in case of water impact and range up to 0.70% (Fig. 10c).

The deformation paths show a very strong impact of **salt solutions** on the strength and general stability of the rock structure. The total compression strength (R_c) is strongly reduced (up to 50% comparing with the natural state) but despite this fact the final, postfailure, residual strength range of 20% of total compression strength (R_c) is continued. The postfailure phase of deformation curves in the vicinity of the pick point show great complexity caused by brittle fracturing interrelated with the short phase of the strengthening processes in the presence of salt incrustation (Fig. 11a). Then the deformation path descends gradually with many symptoms of irregular displacement (Fig. 11b).

The prefailure deformation phases after the effect of salt solutions are characterised by a very short phase of compaction (I) — range up to 3 Mpa, then full linear deformation up to 6 Mpa (II) and then phases of initial, brittle fracturing (III) and phases of stable fracturing (IV), both range up to 10 Mpa and then there is a rapid onset of the phase of unstable deformation (V) — close to 80% of total compression strength (R_c). It is very characteristic for salt solution impact that the critical axial strain (E_z), critical circumferential strain (E_{xy}) and volumetric strain (E_v) are very low (Fig. 11c).

Laboratory testing strength testing results thus show the complexity of the impact of various deterioration factors on the Maadi Town limestone structure and on mechanisms of its deterioration. In processes of swelling and expanding, the immersion in water and temperature changes produced, in the limestone structure, not only brittle cracking defects as is common for salt crystallization, but also ductile deformation and, importantly increasing anisotropy of the rock. Therefore the critical strain values are higher then in case of the salt solution impact when only cracking is involved, and are also more inhomogeneous. Therefore the instability mobilisation factor

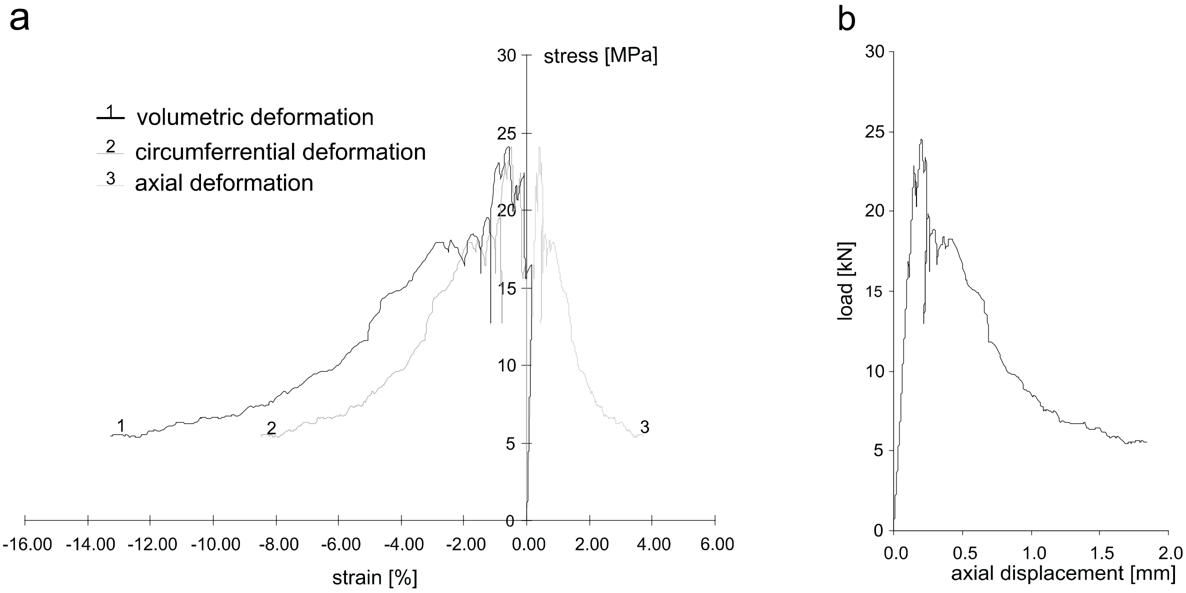

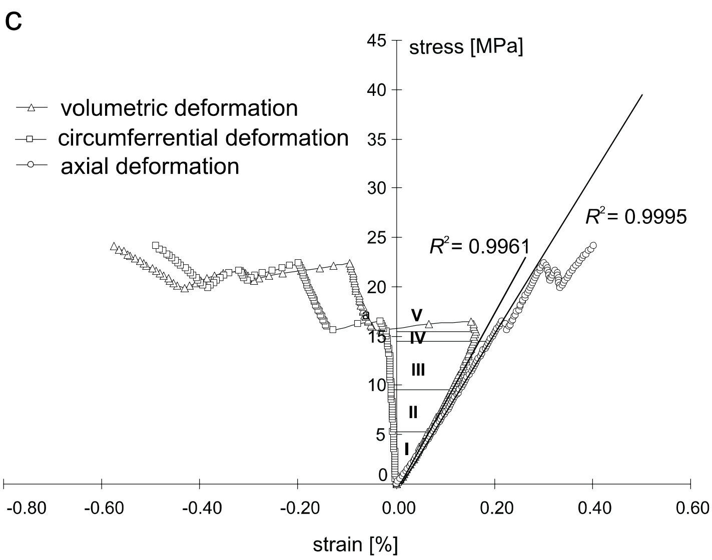

Uniaxial compression strength [Mpa]	Constants of elasticity [10^4 MPa] E	K	G	L	Poisson ratio
24.1	0.80	0.27	0.40	0.05	0.05

Phases deformation — stress threshold									
$\sigma_{I/II}$		$\sigma_{II/III}$		$\sigma_{III/IV}$		$\sigma_{IV/V}$		σ_{bif}	
[MPa]	R_c [%]	[MPa]	R_c [%]	[MPa]	R_c [%]	[MPa]	R_c [%]	[MPa]	R_c [%]
5	22	10	39	15	60	16 16 *	64 64 *	16	67

strain [%] axial						circumferential		
$\varepsilon_{z\ I/II}$	$\varepsilon_{z\ II/III}$	$\varepsilon_{z\ III/IV}$	$\varepsilon_{z\ IV/V}$	ε_{bif}	$\varepsilon_{z\ cr}$	$\varepsilon_{xy\ I/II}$	$\varepsilon_{xy\ II/III}$	$\varepsilon_{xy\ cr}$
0.08	0.13	0.19	0.20	0.22	0.40	-0.01	-0.01	-0.49

volumetric			
$\varepsilon_{v\ I/II}$	$\varepsilon_{v\ II/III}$	$\varepsilon_{v\ IV/V}$	$\varepsilon_{v\ cr}$
0.06	0.11	0.16	-0.58

Fig. 8. Deformation path of Maadi Town Temple limestone in natural state (non-treated samples from Temple construction)

a — full characteristics of prefailure and postfailure axial, circumferential and volumetric characteristics; b — magnification of prefailure axial characteristic; c — numerical analyses of prefailure phase of deformation and calculation of geomechanical parameters I–V, bif — phases of deformation

for such complex mechanisms of structural deterioration is difficult to control.

It may be interpreted and controlled only by using the energy criterion, which is easy to interpret from full curves of deformation. For the limestone analysed the prefailure and postfailure energy indices, after the method given by Pinińska and Bogdańska (Bogdańska, 1999) show that energy of the Maadi Town Temple limestone before reaching a critical stress value (R_c) range up to 20% of the total energy. The energy of microcracks range from 3–7 kJ/m^3 and the energy of macrocracks range up to 11–39, kJ/m^3 while the potential energy decreases due to the impact of water saturation and salt solution (Table 1). Those results compare well with the strength decreases.

CONCLUSIONS

1. The Maadi Town Temple stone construction has been submitted to differential internal and external stresses due to the complex climatic conditions and the varying composition of the limestone material. The ultrasonic tests and destructive geomechanical compressions tests of the building materials, considering the prefailure and postfailure paths of deformation, give the possibility of analysing the mobilisation factor of bearing capacity which causes the total process of stone degradation.

2. The limestones used as a construction material for Maadi Town Temple are inhomogeneous and anisotropic materials,

Table 1

The prefailure and postfailure energy distribution of the building limestone from Maadi Town Tample

Degradation factor	Potencial energy [kJ/m^3]	Prefailure energy	Postfailure energy	Energy index	Macrocracks energy	Microcracks energy	Disperse energy
After drying in 105°C	346	57	289	0.19	18	3	17
Full saturation of water	224	37	187	0.19	45	4	18
After 11 cycles soilsolution	232	28	204	0.14	11	3	14
After 25 cycles soilsolution	166	27	139	0.19	39	7	14

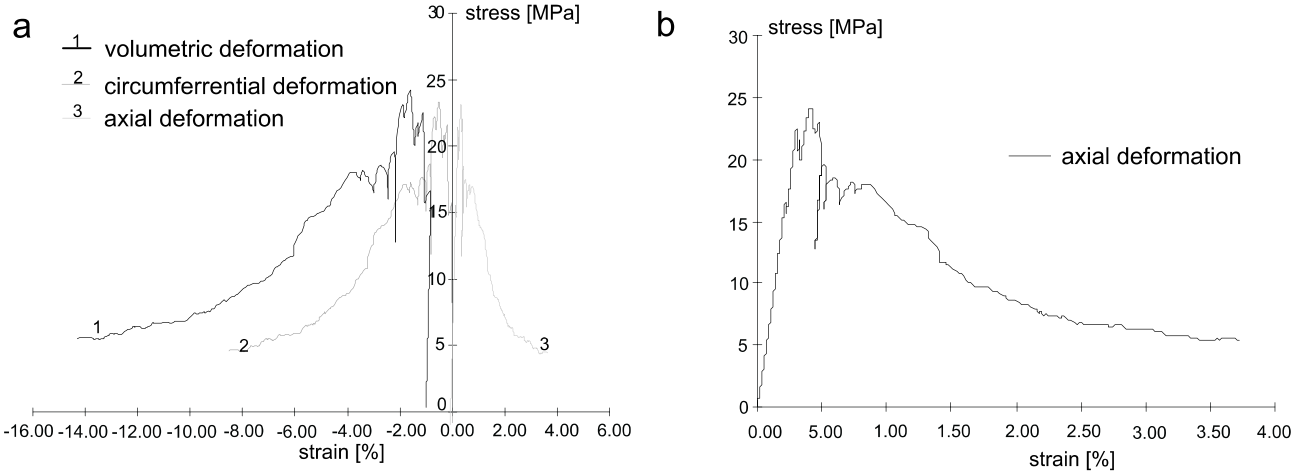

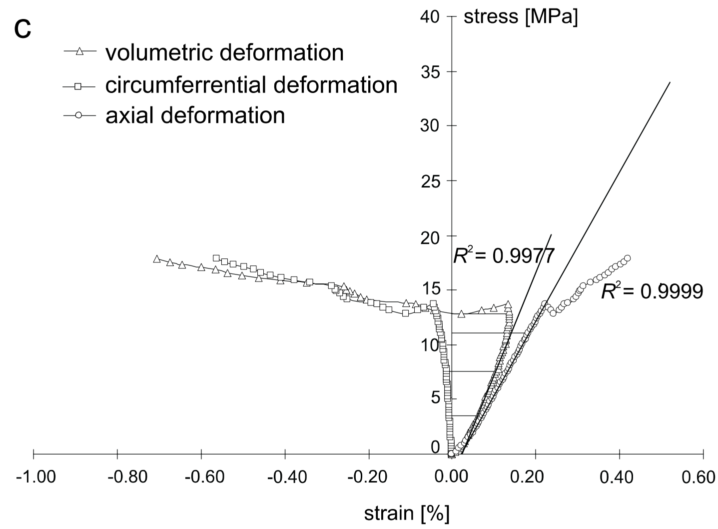

Uniaxial compression strength [Mpa]	Constants of elasticity [10^4 MPa] E	K	G	L	Poisson ratio
17.9	0.69	0.23	0.34	0.11	0.13

Phases deformation – stress threshold

$\sigma_{I/II}$ [MPa]	$\sigma_{I/II}$ R_c [%]	$\sigma_{II/III}$ [MPa]	$\sigma_{II/III}$ R_c [%]	$\sigma_{III/IV}$ [MPa]	$\sigma_{III/IV}$ R_c [%]	$\sigma_{IV/V}$ [MPa]	$\sigma_{IV/V}$ R_c [%]	σ_{bif} [MPa]	σ_{bif} R_c [%]
4	20	8	42	11	62	13 13*	72 72*	13	72

strain [%]

axial $\varepsilon_{z\,I/II}$	$\varepsilon_{z\,II/III}$	$\varepsilon_{z\,III/IV}$	$\varepsilon_{z\,IV/V}$	ε_{bif}	$\varepsilon_{z\,cr}$	circumferential $\varepsilon_{xy\,I/II}$	$\varepsilon_{xy\,II/III}$	$\varepsilon_{xy\,cr}$
0.07	0.13	0.18	0.21	0.24	0.42	-0.01	-0.01	-0.56

volumetric $\varepsilon_{v\,I/II}$	$\varepsilon_{v\,II/III}$	$\varepsilon_{v\,IV/V}$	$\varepsilon_{v\,cr}$
0.06	0.11	0.14	-0.70

Fig. 9. Deformation path of Maadi Town Temple limestone after immersion in water

a — fulI characteristics of prefailure and postfailure axial, circumferential and volumetric characteristics; b — magnification of prefailure axial characteristic; c — numerical analyses of prefailure phase of deformation and calculation of geomechanical parameters I–V, bif — phases of deformation

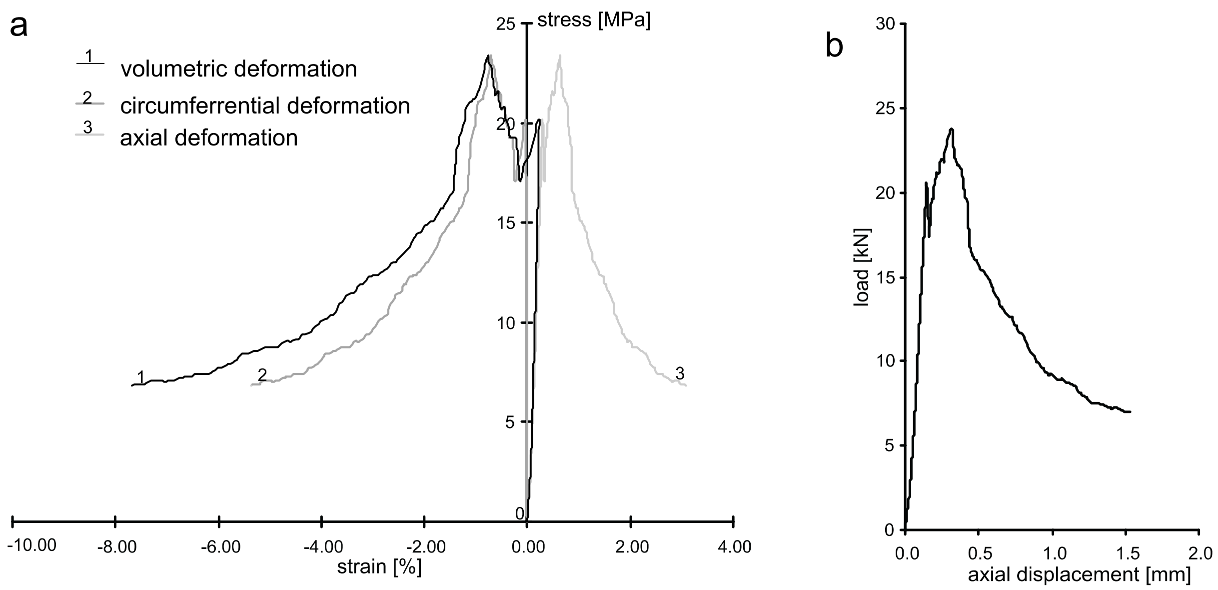

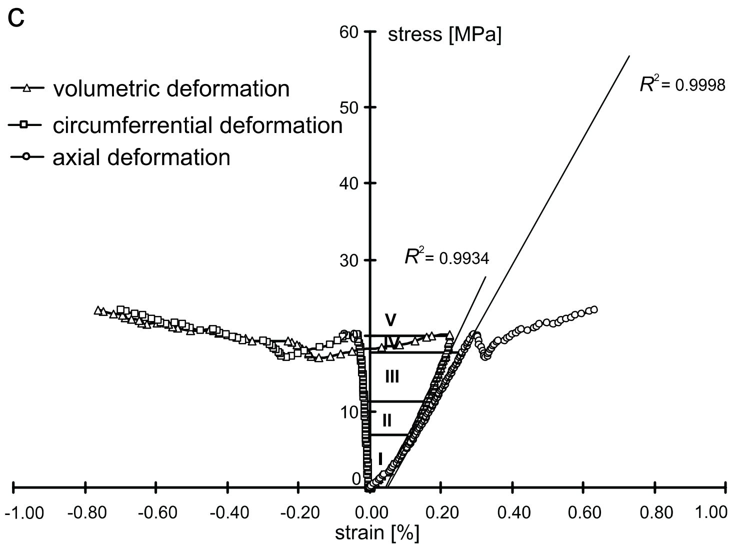

Uniaxial compression strength [Mpa]	Constants of elasticity [10^4 MPa] E	K	G	L	Poisson ratio
23.4	0.83	0.28	0.42	0.08	0.09

Phases deformation – Stress threshold									
$\sigma_{I/II}$		$\sigma_{II/III}$		$\sigma_{III/IV}$		$\sigma_{IV/V}$		σ_{bif}	
[MPa]	R_c [%]	[MPa]	R_c [%]	[MPa]	R_c [%]	[MPa]	R_c [%]	[MPa]	R_c [%]
7	30	11	48	18	76	20 20 *	85 85 *	18	79

strain [%] – axial						strain [%] – circumferential		
$\varepsilon_{z\ I/II}$	$\varepsilon_{z\ II/III}$	$\varepsilon_{z\ III/IV}$	$\varepsilon_{z\ IV/V}$	ε_{bif}	$\varepsilon_{z\ cr}$	$\varepsilon_{xy\ I/II}$	$\varepsilon_{xy\ II/III}$	$\varepsilon_{xy\ cr}$
0.13	0.19	0.26	0.29	0.31	0.63	-0.01	-0.01	-0.70

volumetric			
$\varepsilon_{v\ I/II}$	$\varepsilon_{v\ II/III}$	$\varepsilon_{v\ IV/V}$	$\varepsilon_{v\ cr}$
0.12	0.16	0.23	-0.76

Fig. 10. Deformation path of Maadi Town Temple limestone after temperature cycles (25 cycles)

a — fulI characteristics of prefailure and postfailure axial, circumferential and volumetric characteristics; b — magnification of prefailure axial characteristic; c — numerical analyses of prefailure phase of deformation and calculation of geomechanical parameters I–V, bif — phases of deformation

causing, under the impact of climatic, cyclic changes, high internal stresses inside the rock structure and external stress as between exposed surfaces of heated and cooled rock. Portland cement also leads to internal stress due to the differences in its properties. The inhomogeneous fields of stress increased also due to halite crystals precipitating alongs sedimentary laminae, caused breaking of interlayer bonds.

3. The ultrasonic method of the rock analysis is very useful for monitoring the dynamic changes of stone structure with time due to the impact of deterioration factors. The changes in properties are very rapid initially and and gradually decrease while simultaneously the coefficient of acoustic anisotropy (*Ac*) increases with time due to greater decay parallel to layering than perpendicular to it.

5. The bearing capacity of the stone material of Maadi Town Temple is noticeably reduced as a consequence of cyclic crystallization of salts, development of cracks and crumbling during the temperature cycle because of thermal expansion and contraction, which leads to the development of more cracks and to the disintegration of the internal structure. Various mechanisms of deterioration processes are visible on the paths of deformation and according to their interpretation those most responsible for brittle strength degradation are salt solutions while temperature and water impact play an important role in

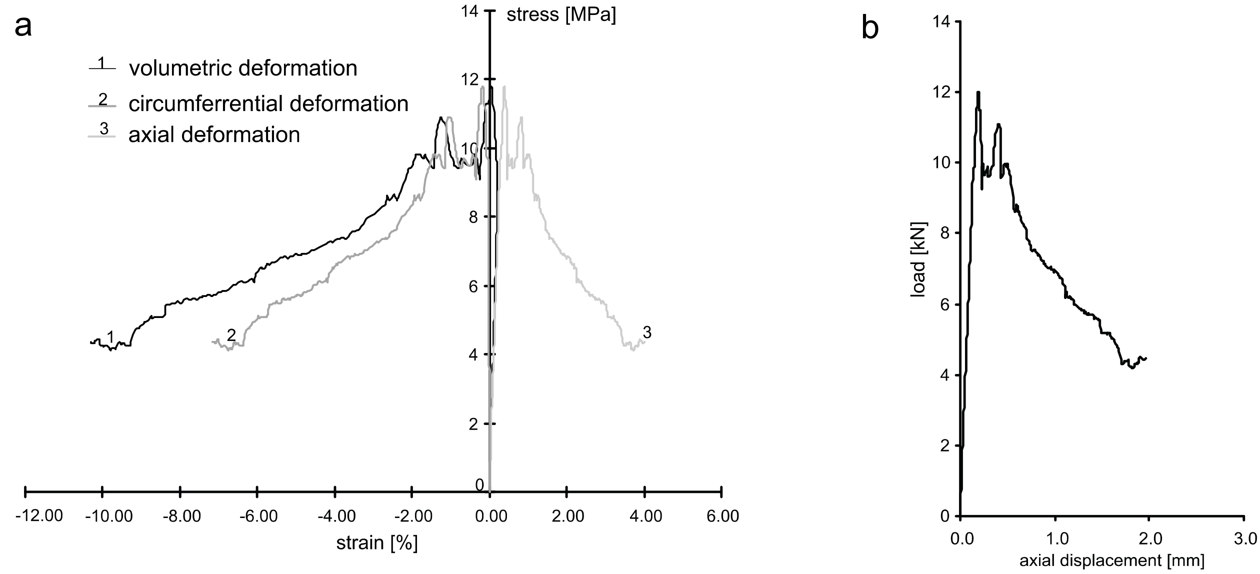

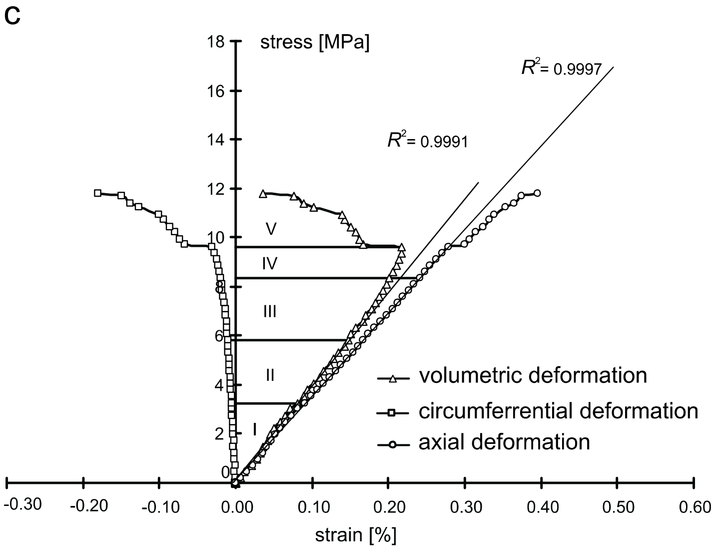

Uniaxial compression strength [Mpa]	Constants of elasticity [10^4 MPa] E	K	G	L	Poisson ratio
11.8	0.34	0.11	0.17	0.03	0.07

Phases deformation — Stress threshold

$\sigma_{I/II}$ [MPa]	$\sigma_{I/II}$ R_c [%]	$\sigma_{II/III}$ [MPa]	$\sigma_{II/III}$ R_c [%]	$\sigma_{III/IV}$ [MPa]	$\sigma_{III/IV}$ R_c [%]	$\sigma_{IV/V}$ [MPa]	$\sigma_{IV/V}$ R_c [%]	σ_{bif} [MPa]	σ_{bif} R_c [%]
3	28	6	49	8	71	10	81	-	-

strain [%]

axial $\varepsilon_{z\,I/II}$	$\varepsilon_{z\,II/III}$	$\varepsilon_{z\,III/IV}$	$\varepsilon_{z\,IV/V}$	ε_{bif}	$\varepsilon_{z\,cr}$	circumferential $\varepsilon_{xy\,I/II}$	$\varepsilon_{xy\,II/III}$	$\varepsilon_{xy\,cr}$
0.09	0.17	0.24	0.28	-	0.40	0.00	-0.01	-0.18

	volumetric $\varepsilon_{v\,I/II}$	$\varepsilon_{v\,II/III}$	$\varepsilon_{v\,IV/V}$	$\varepsilon_{v\,cr}$
-	0.08	0.15	0.22	0.04

Fig. 11. Deformation path of Maadi Town Temple limestone after salt solution cycles (25 cycles)

a — full characteristics of prefailure and postfailure axial, circumferential and volumetric characteristics; b — magnification of prefailure axial characteristic; c — numerical analyses of prefailure phase of deformation and calculation of geomechanical parameters I–V, bif — phases of deformation

increasing the anisotropy of stresses and delay processes of brittle cracking by swelling and expansion.

6. A geomechanical study of the impact of the factors shows the nature of the process of degradation and their role in softening the supporting stone elements of the construction and of the entre construction itself. From the conservation point of view at Maadi Town Temple, it is very important that, despite the low resistance of the building limestone and the high effects of their climatic deterioration, the limestones maintain their postcritical residual bearing capacity at a level of 20% of total compressional strength. If not the total stability of the construction would be rapidly lost.

REFERENCES

ABD EL-HADY M. (2000) — The deterioration of Nubian sandstone blocks in the ptolemaic temples in Upper Egypt. In: Proceeding of the 9th International Congress on Deterioration and Conservation of Stone. Venice June 19–24. Elsevier, **2**: 783–792. Amsterdam.

ATTIA H. R. (1995) — Study of treatment and conservation of Seti I Temple and Memorial Tomb (Osireion) in Abydous area. M. Sc. Thesis. Archives of Architecture Faculty of Cairo University. Cairo.

BEADNELL H. J. (1905) — The topography and geology of the Fayoum Province of Egypt. Nat. Print. Depart. Cairo.

BOGDAŃSKA J. (1999) — Energy of deterioration as a criterion of the cracking processes control — an example for reservoir rocks of Lublin region, Poland (in Polish). Ph. D. Thesis. Department of Geomechanics. Warsaw University.

HELMI F. M. and ATTIA H. R. (1996) — Characterization and conservation of Seti I Temple. Abydous. Upper Egypt. In: Proceeding of the 8th International Congress on Deterioration and Conservation of Stone. Berlin. Balkema, **2**: 1123–1136. Rotterdam. Brookfield.

HEWISANN R. N. (1986) — The Fayoum. The American University. Cairo.

HOEK E. and MARINOS J. (2001) — Estimating the geotechnical properties of heterogeneous rock masses such as flysch. Bull. IAEG. Springer-Verlag, **60** (2): 85–92.

PINIŃSKA J. (1995) — Crack growth in the postcritical path of deformation of sedimentary rocks. In: Proceedings of the Second International Conference on the Mechanics of Jointed and Faulted Rock. Vienna. 10–14 April. Balkema: 113–118. Rotterdam. Brookfield.

PINIŃSKA J. (1999) — Deformation and strength properties of rocks (in Polish). (III/5). Ed. Zakład Geomechaniki. I.H.G.I. UW. Warszawa.

PINIŃSKA J. and ATTIA H. R. (1999*a*) — Study of the building materials of Maadi Town Temple. Fayoum. Egypt. In: Proceedings of 6th International Conference on Non-Destructive Testing and Microanalysis for the Diagnostics Conservation of the Cultural and Environmental Heritage. May 17–20, Rome, **1**: 619–632.

PINIŃSKA J. and ATTIA H. R. (1999*b*) — Mechanical and thermal weathering problems of the Maadi Town Temple, Fayoum, Egypt. In: Proceedings of the 9th International Congress on Rock Mechanics. Paris. August 25–28. Balkema: 1011–1014. Rotterdam. Brookfield.

SAID R. (1962) — The geology of Egypt. New York.

WOLFGANG H. and EBERHARD O. (1979) — Lexikon der Agylote. Otto Harrassowitz: 1271–1273. Wiesbaden.